Eur Food Res Technol (2005) 220:587–591
DOI 10.1007/s00217-004-1102-3

ORIGINAL PAPER

Hongshun Yang · Hongjie An · Guoping Feng · Yunfei Li · Shaojuan Lai

Atomic force microscopy of the water-soluble pectin of peaches during storage

Received: 4 August 2004 / Revised: 3 November 2004 / Published online: 8 January 2005
© Springer-Verlag 2005

Abstract Yellow peaches (*Prunus persicu* L. Batsch.) were stored under a controlled atmosphere of 2% O_2 + 10% CO_2, or a normal atmosphere at 2 °C, in order to investigate the effects of storage conditions, atmosphere and time on the structure of a single water-soluble pectin (WSP) molecule. The microstructural changes of the branches and widths of WSP were studied by atomic force microscopy (AFM) on the 1st, 15th and 45th days under the assigned atmosphere. The probability of small-width WSP increased with time in both groups, but the probability was larger in the normal-atmosphere group. The microstructure of WSP molecules and polymers showed that the aggregate separation increased with storage time. The degradation of WSP molecules was inhibited by controlled-atmosphere storage. The majority of the chains were composed of four basic units with widths of 11.719, 15.625, 19.531 and 35.156 nm, which could be visualized and calculated exactly by AFM. These results indicate that parallel linkages or intertwists between the basic units are fundamental conformations for WSP molecules.

H. Yang
Institute of Refrigeration & Cryogenics Engineering,
Shanghai Jiao Tong University,
Shanghai, 200030, China

H. An
Nanobiology Laboratory,
Shanghai Jiao Tong University,
Shanghai, 20030, China

H. Yang · G. Feng · Y. Li (✉)
Department of Food Science & Technology,
Shanghai Jiao Tong University,
2678 Qixin Road, Shanghai, 201101, China
e-mail: yfli@sjtu.edu.cn
Tel.: +086-21-64783085
Fax: +086-21-64783085

S. Lai
The Third Xiangya Hospital,
Central South University,
Changsha, 410013, China

Keywords Peach · Atomic force microscopy · Controlled-atmosphere storage · Pectin · Structure

Introduction

Plant pectin is a very important foodstuff and additive to food products. It is a family of complex galacturonic acid-rich polysaccharides present in the primary cell wall and intercellular spaces of higher plants [1]. Its common compositions are homogalacturonan (HG), rhamnogalacturonan I (RG-I), rhamnogalacturonan II (RG-II) and xylogalacturonan. The functional properties of pectin, at both harvest and postharvest time, are closely related to its chemical and physical structures. Classical methods, like NMR [2], the enzyme method [1, 3], and the biochemistry method [4], have been used to detect the structures.

The degradation of pectin is important for commercial application [5]. However, since pectin has a heterogeneous structure, sit is difficult to study the molecular structure. Varied structures or complex repeat units are not easily determined owing to the irregular sequences that tend to be averaged across the whole sample with most techniques.

Atomic force microscopy (AFM) affords an opportunity to directly image individual pectin molecules and polymers. Sodium carbonate soluble pectin from unripe tomatoes [6, 7], alginate and gels [8], biopolymers [9], ι-carrageenans [10], and cell walls [11, 12] have been studied by AFM. The molecular branching, molecular mass distributions, interactions involved in supramolecular assembly, cell wall structure, and polysaccharide gelatin have been illustrated in these works.

Controlled-atmosphere (CA) storage is important for maintaining a high quality of produce, including firmness [13]. Produce texture is related to pectin [14, 15]; however, there are no reports about the degradation of pectin under CA storage by AFM. To demonstrate and further illustrate the effects of enzymes on pectin and to compare the results with enzymatic research [1, 3, 4], we chose

water-soluble pectin (WSP) as an analysis object because it is involved in complex reactions and is not easily studied by chemical methods.

The overall goal of this study was to examine the morphological arrangement of peach WSP and its changes during storage. The degradation mechanism of the peach pectin was also studied by AFM images.

Materials and methods

Fruits

Yellow peaches (*Prunus persicu* L. Batsch.) at commercial maturity, according to acceptable color standards, were harvested from an orchard in Fengxian, Shanghai City, China. The fruits were transported to a laboratory within 2 h of harvest and precooled (4 °C, 12 h) immediately upon arrival. They were stored at 2±1 °C until testing time.

Storage conditions

The storage conditions were as follows: CA, 2% O_2 + 10% CO_2, and normal atmosphere (CK). Two CA cabinets (105 cm× 55 cm×100 cm) with two CO_2 absorbers (soda lime containing ethyl violet as an indicator) and two ethylene absorbers were connected to an atmosphere analyzer (GAC 1100, Italy). The initial concentrations of O_2 and CO_2 in the CA and CK cabinets were established by control of the flow rate of N_2 generated by the cellulose membrane and CO_2 via pressure regulators. There was 120±10 kg of peaches in each cabinet and all treatments were at 2±1 °C with approximately 95% relative humidity (RH).

WSP extraction

The WSP was extracted according to the method of Zhou et al. [16] with slight modifications. Peaches taken from CA and CK groups were peeled and about 5.5 g flesh from each storage condition was used for extraction of cell wall material. The flesh was boiled in ethanol for 20 min, the ethanol was decanted by filtration, and the solid residue was transferred to 20 ml ultrapure water (Milli-Q Biocel Pure Water Equipment, Millipore Co., France). After a 2-h extraction, the supernatant was collected by centrifugation (Beijing Medical Equipments Co.) at 15,000*g* for 10 min. The samples were refrigerated until analyzed.

AFM manipulation

AFM in a glove box was carried out at 30–40% RH and 23–25 °C. The variation of humidity inside the glove box was controlled by silica gel and stabilized for at least 5 h prior to AFM observation [17].

Pectin solutions were recovered to room temperature and were diluted to 0.5–30 μg/ml with serial dilutions of the concentrations. To deposit WSP solutions (after a strong dispersion) onto newly cleaved sheets of mica, a small volume (20 μl) of the solutions was pipetted briefly (about 5 s) onto the mica surface, and then quickly removed by pipetting. The mica surface was air-dried (1 h) in a dust-free enclosure, before using AFM imaging with tapping mode at a scan speed of about 2 Hz.

Tapping mode was carried out using a multimode NanoScope IIIa atomic force microscope (Digital Instruments, USA) equipped with a Si_3N_4 cantilevered scanner with a 12×12-μm^2 scan size and a 4-μm vertical range. The possible scan size is larger than the area of the final pictures. The scanner can move to suitable places to get satisfactory pictures. In the tapping mode atomic force microscope, the tip was oscillated with a high frequency in the vertical direction and was only intermittently in contact with the sample. It has a high resolution of about 0.1 nm for the vertical range and 1–2 nm for the lateral range [18]. To make the results comparable, before imaging each sample the integrity of the AFM tip was verified by imaging a reference standard with a known roughness of 5–7 nm [19].

Since AFM images are generally limited to small scanned areas, several images of different zones were examined and analyzed offline with version 5.12 of the software for each specimen in order to average the results [18]. The correction of the images by this software enabled us to reduce the noise of the samples.

AFM image analysis

The bright and dark areas in the image correspond to peaks and troughs in the WSP chains. Different scales were used in the vertical and horizontal scales, with the height mode being used for the analysis.

The intervals of aggregates and single molecules were measured by section analysis. In this analysis, the image was sectioned along a line orthogonal to the direction of the samples and the surface profile of the section was plotted. From this surface profile, the width of the sample could be calculated. The length distribution of the molecules can now be plotted throughout the measurements of the single molecules [20].

Branched structures were distinguished from overlapping molecules by measuring the heights of the chains. In general, the heights of the chains rose twofold when two chains crossed over one another. At genuine branch points the height remained unchanged [21].

The width of a single strand can be calculated by the horizontal distance (*L*) with the software and the height of the chain can be calculated by the vertical distance (*V*). The number of times the chain widths occurred was recorded as the frequency.

Statistical analysis

Statistical analysis of WSP chain widths through analysis of variance ($P<0.05$) and Duncan's multiple range tests was performed using SAS 8.0.

Results and discussion

Effects of atmosphere and time on WSP structures and aggregates

The high resolution of the atomic force microscope offers the potential for characterizing the heterogeneous structures of WSP, including linear, branching, blocks, or polymers.

Figure 1 shows the AFM images of WSP from a fresh peach. Figures 2 and 3 show typical images of WSP from a peach on the 15th day of storage under CA and CK. Figures 4 and 5 show the images of the two groups on the 45th day.

Aggregated polymers and polymers too small to be exactly visualized with the software were excluded from the statistical analysis. The statistical results were calculated from dozens of images. Frequency and *V* values of different chain widths (*L*) of different storage times and atmospheres are shown in Tables 1, 2, and 3. Table 1 shows the results of initial storage, and Tables 2 and 3 show the CA and CK groups after 15 and 45-days' storage, respectively.

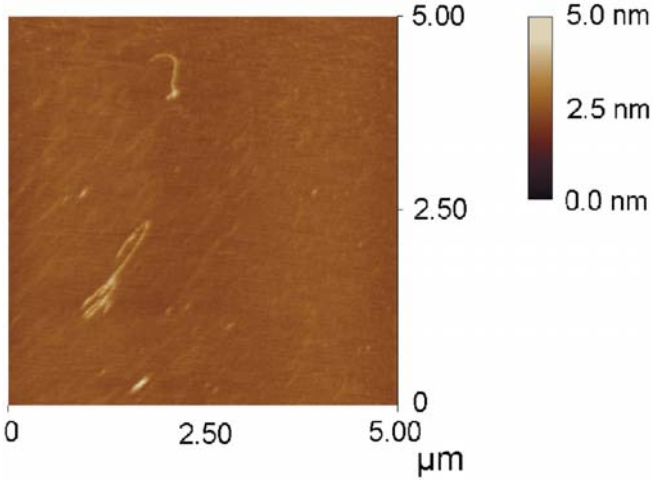

Fig. 1 Atomic force microscopy (*AFM*) image of water-soluble pectin (*WSP*) from a fresh peach.

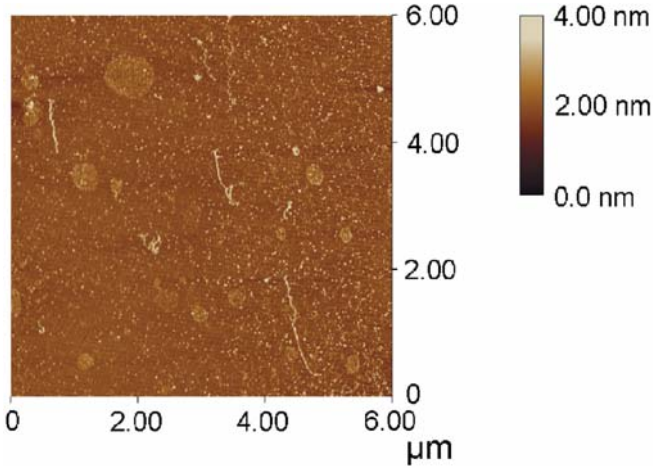

Fig. 3 AFM image of WSP from a peach on the 15th day under normal-atmosphere (*CK*) storage.

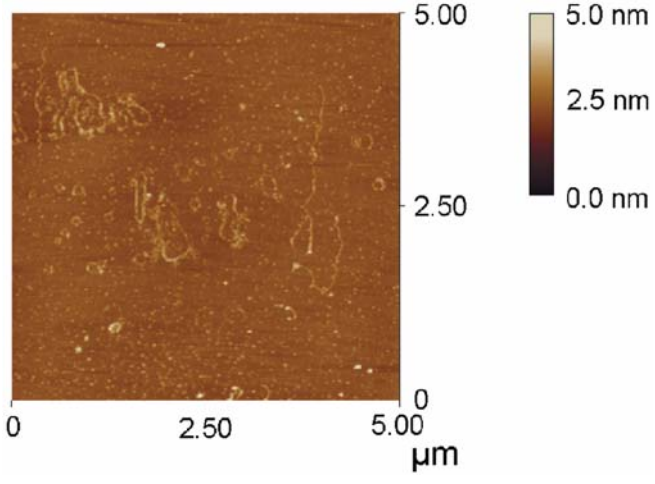

Fig. 2 AFM image of WSP from a peach on the 15th day under controlled-atmosphere (*CA*) storage.

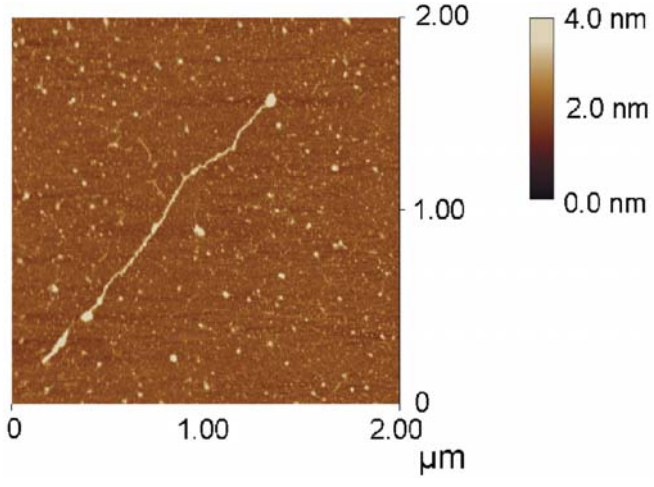

Fig. 4 AFM image of WSP from a peach on the 45th day under CA storage.

From the three tables, it is clear that the probability of smaller *L* value chains was higher in the CK group than in the CA group. On the 15th day of storage, a width of 58.594 nm was measured three times and a width of 39.063 nm was measured six times in the CA group; however, these widths appeared only once in the CK group, as shown in Tables 1 and 2. The phenomenon was similar on the 45th day. These results indicate that CA storage inhibited the degradation of the linkage between the WSP molecules, which resulted in the smaller widths. The probability of this occurring increased with time in the same group. There was no statistical significance for *V* values and the lengths of chains.

The width of the chains from section analysis reflected a group of basic units, with widths of 11.719, 15.625, 19.531, and 35.156 nm, and the widths of other types of chains can be composed of these four values. For example, 58.594 nm is the sum of 35.156 and 23.438 nm, and 97.656 nm is approximately the sum of 58.594 and 39.063 nm. Values 23.438, 35.156, and 78.125 nm are twice the size of 11.719, 17.578, and 39.063 nm, respectively.

Decho [8] reported that scleroglucan had a single-strand polymer with a width of 0.55 nm based on X-ray diffraction measurements; however, the width of scleroglucan was found to be 1 nm by AFM. The differences may be due to a probe-broadening effect or side-by-side association of molecules. Adams et al. [21] suggested that the discrepancy might partly be a result of formation of the helical structure. The purely geometrical effect can be estimated by calculating the radius (r) of a cylindrical molecule whose measured width (w) is broadened by a tip of radius R, using the relationship $r = w^2/16R$. For example, suppose the measured width of the pectin was around 15 nm and the tip radii lay between 20 and 40 nm, a range of molecular rods would be calculated between 0.35 and 0.7 nm in radius [22].

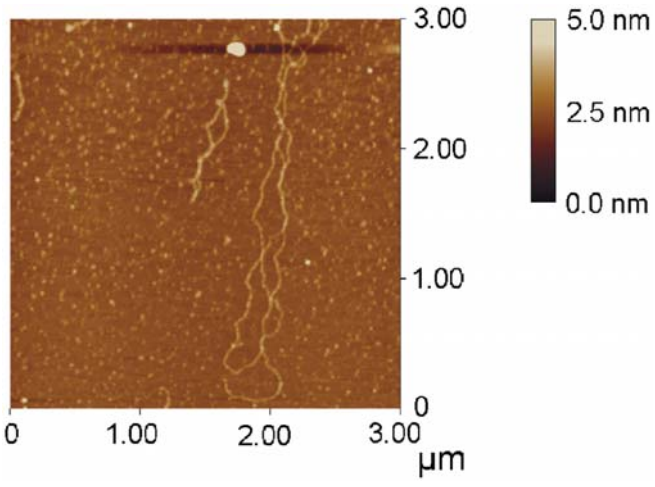

Fig. 5 AFM image of WSP from a peach on the 45th day under CK storage.

Table 1 Frequency (*Fq*) and vertical distances (*V*) of water-soluble pectin (*WSP*) chain widths (*L*) at the initiation of storage.

L (nm)	Fq	*V* (nm)
97.656	1	1.847±0
78.125	2	1.637±0.528
58.594	9	1.203±0.338

Table 2 Frequency and vertical distances of WSP chain widths under controlled-atmosphere storage.

L (nm)	15th day		45th day	
	Fq	*V* (nm)	Fq	*V* (nm)
58.594	3	1.742±0.146	0	0±0
39.063	6	0.967±0.112	0	0±0
35.156	2	1.092±0.293	4	2.421±0.824
23.438	2	1.021±0.032	0	0±0
19.531	1	0.656±0	3	1.714±0.486
15.625	0	0±0	2	1.791±0.001
11.719	0	0±0	1	1.660±0

Table 3 Frequency and vertical distances of WSP chain widths under normal-atmosphere storage.

L (nm)	15th day		45th day	
	Fq	*V* (nm)	Fq	*V* (nm)
58.594	1	1.496±0	0	0±0
39.063	1	1.552±0	0	0±0
35.156	6	1.516±0.411	6	1.250±0.256
23.438	0	0±0	5	1.154±0.213
19.531	0	0±0	0	0±0
15.625	1	0.963±0	0	0±0
11.719	1	1.248±0	2	0.897±0.057

The aggregates were present even at low dilutions of a few single polymers, which suggested that they are not simply superpositions or entanglements of polymers caused by the reduction of solvent volume during drying down to the substrate. The characteristic of a single polymer was different from that of multipolymers [7].

Mechanism of the structural changes of WSP molecules

For the heterogeneous and complex structure, it has been difficult to explore the changes of pectin structure during storage. In recent years, many researchers have investigated the structure of pectin through specific enzyme actions. Limberg et al. [1] compared the actions of plant-pectin methylesterase (p-PME) and fungal-pectin methylesterase (f-PME). Herbert et al. [23] proposed that pectin was initially secreted in a highly methylated form and only later became de-esterified within the cell wall by PME, with the cell wall penetration involving enzymatic activity rather than mechanical force.

Massio et al. [24] observed that the initial attack of PME was endo and allowed polygalacturonase action within the galacturonic chain. In our experiments, on the 45th day of storage many of the WSP molecules were linear without branches. Further work needs be done to explore whether selective cleavage happened, because selective cleavage of unesterified galacturonic acid residues allows the side chains to be released from the molecule [25].

Many scholars agree that p-PME causes blockwise de-esterification of pectin, whereas f-PME typically causes random de-esterification [1, 5]. Morris et al. [26] suggested that the decrease in molecular weight was due to chain cleavage from β-elimination and that the increase of the reaction time for the neutral protocol resulted in increased cleavage. Ridley et al. [5] proposed that HG and RG-II were probably covalently linked since they both had backbones composed of 1,4-linked α-D-GalpA residues and treating cell walls with endopolygalacturonase solubilized them both. However, there is much evidence that suggests that RG-I is not linked to other backbones, and there is a substantial body of data showing that RG-II molecules are covalently cross-linked by borate esters.

In our experiments, the probability of WSPs having widths of small values increased with the storage time, which indicated the decrease of width is an important phenomena for WSP structures. The widths are four basic units of 11.719, 15.625, 19.531, and 35.156 nm, which were obtained from AFM. This indicates that parallel linkages or intertwists between the basic units are fundamental information for the structure of the WSP molecule, most likely between HG and RG-II components [5]. Moreover, CA storage could inhibit the degradation of the linkage between the WSP molecules.

Conclusions

CA with lower O_2 and higher CO_2 concentrations inhibited the degradation of WSP of peach pectin as visualized by AFM. The widths of WSP are composed of four basic units: 11.719, 15.625, 19.531, and 35.156 nm, which can

be visualized by AFM. These results indicate that parallel linkages or intertwists between the basic units are fundamental information for WSP molecules.

Acknowledgements This research was supported by grants from the National Economy and Commence Committee (project no. 02CJ-12-07-03). The first two authors contributed equally to this article.

References

1. Limberg G, Körner R, Buchholt HC, Christensen TM, Roepstorff P, Mikkelsen JD (2000) Carbohyd Res 327:293–307
2. Golovchenko VV, Ovodova RG, Shashkov AS, Ovodov YS (2002) Phytochem 60:89–97
3. Limberg G, Körner R, Buchholt HC, Christensen TM, Roepstorff P, Mikkelsen JD (2000) Carbohyd Res 327:321–332
4. Vetter S, Kunzek H (2003) Eur Food Res Technol 217:392–400
5. Ridley BL, O'Neill MA, Mohnen D (2001) Phytochem 57:929–967
6. Round AN, MacDougall AJ, Ring SG, Morris VJ (1997) Carbohyd Res 303:251–253
7. Round AN, Rigby NM, MacDougall AJ, Ring SG, Morris VJ (2001) Carbohyd Res 331:337–342
8. Decho AW (1999) Carbohyd Res 315:330–333
9. Morris VJ, Mackie AR, Wilde PJ, Kirby AR, Mills EC, Gunning P (2001) Lebensm Wiss Technol 34:3–10
10. Gunning AP, Cairns P, Kirby AR, Round AN, Bixler HJ, Morris VJ (1998) Carbohyd Polym 36:67–72
11. Kunzek H, Kabbert R, Gloyna DZ (1999) Lebensm Unters F A 208:233–250
12. Fahlén J, Salmén LJ (2003) Mater Sci 38:119–126
13. Artés F, Escalona VH, Artés-Hdez F (2002) Eur Food Res Technol 214:216–220
14. Villarreal-Alba EG, Contreras-Esquivel JC, Aguilar-González CN, Reyes-Vega ML (2004) Eur Food Res Technol 218:164–166
15. Tijskens LM, Rodis PS, Herbog ML, Kalantzi U, Dijk C (1998) J Food Eng 35:111–126
16. Zhou HW, Sonego L, Khalchitski A, Ben-Arie R, Lers A, Lurie S (2000) J Am Soc Hortic Sci 125:630–637
17. Balnois E, Wilkinson KJ (2002) Colloid Surface A 207:229–242
18. Darrort V, Troyon M, Ebothé J, Bissieux C, Nicollin C (1995) Thin Solid Films 265:52–57
19. Reed J, Singer E, Kresbach G, Schwartz DC (1998) Anal Biochem 259:80–88
20. Wada H, Usekura H, Sugawara M, Katori Y, Kakehata S, Ikeda K, Kobayashi T (2003) Hearing Res 177:61–70
21. Adams EL, Kroon PA, Williamson G, Morris VJ (2003) Carbohyd Res 338:71–780
22. Morris VJ, Gunning AP, Kirby AR, Round A, Waldron RK, Ng A (1997) Int J Biol Macromol 21:61–66
23. Herbert C, O'Connell R, Gaulin E, Salesses V, Esquerré-Tugayé MT, Dumas B (2004) Fungal Genet Biol 41:140–147
24. Massiot P, Perron V, Baron A, Drilleau JF (1997) Lebensm Wiss Technol 30:697–702
25. Needs PW, Rigby NM, Ring SG, MacDougall AJ (2001) Carbohyd Res 333:47–58
26. Morris GA, Hromádková Z, Ebringerová A, Malovíková A, Alföldi J, Harding SE (2002) Carbohyd Polym 48:351–359